Three-Dimensional Critical Behavior with 2D, 1D, and 0D Dimensionality Crossover: Surface and Edge Specific Heats

M. O. Kimball, K. P. Mooney, and F. M. Gasparini
Department of Physics
University at Buffalo
State University of New York
Buffalo, NY 14260, USA
(Dated: January 21, 2004)

The critical behavior at a second order phase transition is characterized by the divergence of the correlation length $\boldsymbol{\xi}$. We have studied the superfluid transition of ^{4}He in a series of experimental cells in which this divergence of $\boldsymbol{\xi}$ is modified due to finite-size confinement. In particular, the design of these cells is such that the smallest dimension is kept the same, 1 $\boldsymbol{\mu}$m, but the geometry is such that one obtains crossover to dimensionality of 2, 1, and 0. This corresponds to films, channels and boxes filled with helium. We measure the specific heat, and compare these results with theoretical expectations. We identify surface and line specific heat contributions by analyzing the deviation of the specific heat from its behavior in the thermodynamic limit. The design of these cells is made possible by a combination of silicon lithography, and direct wafer bonding.

The thermodynamic behavior of a system near a second order phase transition is well understood [1]. Singularities are observed in a number of thermodynamic properties. These result from the divergence of the correlation length ξ as the critical temperature T_c is approached. This length scale determines the spacial extent of fluctuations near T_c. While all systems studied are finite in extent, this is not reflected in typical measurements because one does not approach the transition temperature closely enough for ξ to become macroscopic. For typical systems, ξ is of the order of 1 μm at $t \equiv |1-T/T_c| \approx 10^{-6}$. Thus, for samples of much greater dimensions one obtains behavior which is independent of their shape or size. One identifies this as the thermodynamic limit, or bulk behavior.

Alternatively, one may ask how a system with dimensions comparable to ξ reaches the thermodynamic limit as its small dimensions are increased. This represents an important problem in statistical mechanics. This limit can be approached by a confined system in which, at the simplest, one starts with 1, 2, or all 3 spacial dimensions uniformly small. One expects that, for equivalent confinements, one should be able to scale the data with critical exponents which are related to bulk properties [2]. This expectation is often used theoretically in calculations on finite systems and extrapolations to the thermodynamic limit [3]. Finite systems are inherently shape dependent. Thus, to study them, control of the confinement geometry is essential. Further, it is necessary to realize confinement in such a way that walls do not influence the ordering in an essential way.

The transition of liquid ^{4}He from a normal fluid to a superfluid is ideal in many ways for such a study. The ordered state is characterized by a macroscopic wave function, which is often assumed to obey Dirichlet boundary conditions at walls. The local van der Waals field at the walls provides an inhomogeneity which is relatively benign, since it influences the order parameter indirectly and at most over a limited spacial range. Lastly, the critical behavior in the thermodynamic limit is very well known [4]. In the limit in which three, or two of the spatial dimensions of the confined helium are made small, no sharp critical behavior is expected. On the other hand, when only one dimension is small, the case of a film, one expects a Kosterlitz-Thouless (KT) behavior[5]. The challenge in studying finite-size effects is to achieve uniform confinement of the liquid at the μm scale, and to make a high resolution measurement of a relatively small sample.

To achieve uniform confinement we use a combination of lithography and direct silicon wafer bonding [6]. A "cell" consists of two wafers bonded together, thus defining a specific geometry. We use standard optical lithography to pattern SiO_2 grown on a 5 cm wafer. For planar confinement (2 dimensional, 2D crossover) we pattern the oxide with a series of posts 1 μm high, and about 1 mm apart on which the second wafer is then bonded. The posts maintain a uniform separation between the wafers over the full volume of the cell. For 1D crossover we pattern the oxidized wafer with 1 μm $\times$ 1 μm $\times$ 4 mm channels. The experimental cell is tiled with a pattern so that there is about 0.5 km of channels. For 0D crossover the oxide is patterned with an array of 10^9 cylindrical boxes 1 μm high by 1 μm diameter. This latter cell is distinguished from the others by having the top wafer also patterned with shallow, 18.5 nm high, 1 μm wide lines to fill the boxes[7]. Thus, this cell may be reliably regarded as a collection of uncoupled boxes[7]. Further details of our cells can be found in [6, 8]. For all cells, one can deduce the spacing after bonding via a measurement of interference fringes in the infrared. From these, we deduce that the separation is uniform to better than 10 nm across the area of the wafers. This is much better than the free-state flatness of these wafers which can have

variations as large as 10^4 nm. The uniformity is achieved by incorporating a substantial stress in the wafers as they contour to each other in the bonding process.

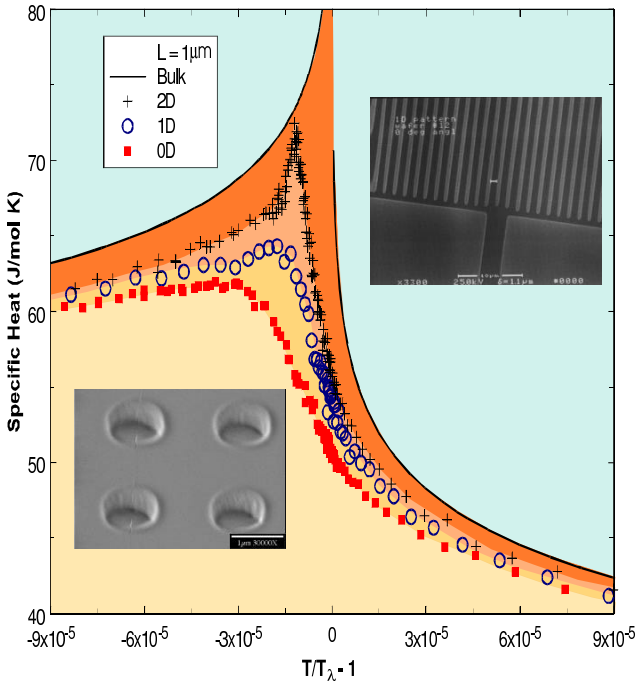

FIG. 1: Specific heat near the superfluid transition of helium confined to a film of thickness L[9], a channel $L \times L$, and a box $L \times L \times L$ all with $L = 1\mu$m. The insets are SEM images of the patterns showing the boxes and the channels. For the latter, a wider channel is shown. This communicates with a filling capillary which brings helium into the cell.

To measure the specific heat of confined helium, a cell is staged on a cryostat in such a way as to allow for the presence of a small amount of bulk helium *outside* the wafers. This yields the bulk transition temperature, T_λ. The heat capacity of the confined helium is determined by measuring the amplitude of the temperature oscillations when the cell is heated with an ac current. This is done at such a frequency, typically 25-40 Hz, whereby the bulk helium, due to its longer relaxation time, does not contribute to the heat capacity. This was checked explicitly [8].

Our data for the specific heat of helium in the neighborhood of the maximum are shown in Fig. 1. The insets on this figure are electron micrographs of the channel and box geometries.The planar geometry may be viewed simply as a film, 1 μm thick and of infinite lateral extent. The specific heats behave qualitatively very much as one might expect. That is, the more one restricts the dimensionality of the system, thereby further limiting critical fluctuations, the weaker the specific heat maximum becomes. Hence the data nest under the solid line, which is the bulk behavior, with a hierarchy of film, channels, and then boxes. Note as well, that the shift in the specific heat maximum also follows the same hierarchy, with the maximum for the boxes undergoing the largest shift.

The expectation for finite-size behavior is that the specific heat for a system confined uniformly to a small dimension L should obey a scaling form which can be cast in several ways [10]. In particular, one may write

$$[C(t,\infty) - C(t,L)]t^\alpha = \Delta C t^\alpha \equiv g_2(x) \qquad (1)$$

where $t = |1 - T/T_\lambda|$. The variable x is $tL^{1/\nu}$. The exponents, $\alpha = -0.0115$ and $\nu = 0.6705$, characterize the singularity in the bulk specific heat $C_p \sim t^{-\alpha}$, and the divergence of the correlation length $\xi \sim t^{-\nu}$. These exponents [11] are well established in helium and are related via the hyperscaling relation $3\nu + \alpha = 2$. The scaling variable, apart from a constant, is simply $(L/\xi)^{1/\nu}$.

An alternative way of representing the data is as [12]

$$[C(t,L) - C(t_0,\infty)]L^{-\alpha/\nu} = f_1(x) \qquad (2)$$

where t_0 is the temperature at which $\xi = L$. These two functions are equivalent, but their different forms are useful because they emphasize different features of the specific heat.

Another approach in describing a finite system is to consider how, in a region where ξ/L is small (far from the transition), it might begin to deviate from bulk behavior. This may be expressed as being due to topological aspects of the confining geometry, such as corners, edges and surfaces [3]. The edge (e) and surface (s) contributions to the full scaling function may be written respectively as,

$$\Delta C t^\alpha \approx -\frac{g_e}{L^2}\frac{A_e}{\alpha_e}t^{\alpha-\alpha_e}, \qquad (3)$$

$$\Delta C t^\alpha \approx -\frac{g_s}{L}\frac{A_s}{\alpha_s}t^{\alpha-\alpha_s}. \qquad (4)$$

These are the dominant contributions in the edge and surface regions of the scaling plots. The surface and edge expressions no longer apply if $tL^{1/\nu}$ becomes small. They are part of the crossover behavior contained in the full scaling function. This differs for each type of confinement. For Eqs. 3,4 to be functions of ξ/L, one must have $\alpha_s = \alpha + \nu$ and $\alpha_e = \alpha + 2\nu$. The amplitude for the surface specific heat, A_s, has been calculated recently [13]. The amplitude for the edge specific heat, A_e, is unknown and, as far as we are aware, has never been measured for a critical system. These amplitudes are *independent of the geometry*. The constants g_s and g_e however, do depend respectively on the surface to volume and edge to volume ratios for a particular geometry. In our case, for films, channels and boxes g_s is 2, 4, and 6, respectively. Similarly, for g_e one has 0, 4, and $8g_0$. This g_0, which is between 0.5 and 1, reflects the uncertainty in the alignment of the filling lines relative to the boxes. According

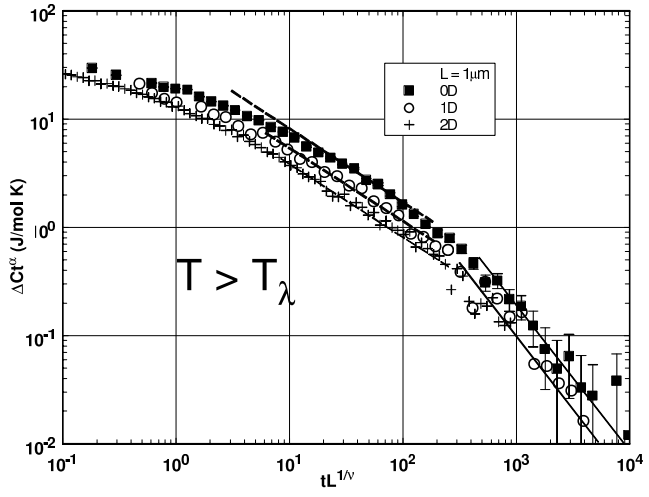

FIG. 2: The difference in the specific heat of confined helium from the bulk for $T > T_\lambda$ plotted according to Eq. 1. The solid lines for large values of $tL^{1/\nu}$ indicate the behavior of the edge specific heat. The dashed lines, at intermediate $tL^{1/\nu}$ indicate the behavior of the surface specific heat. For small $tL^{1/\nu}$ the full effect of confinement is manifest. L is in Å.

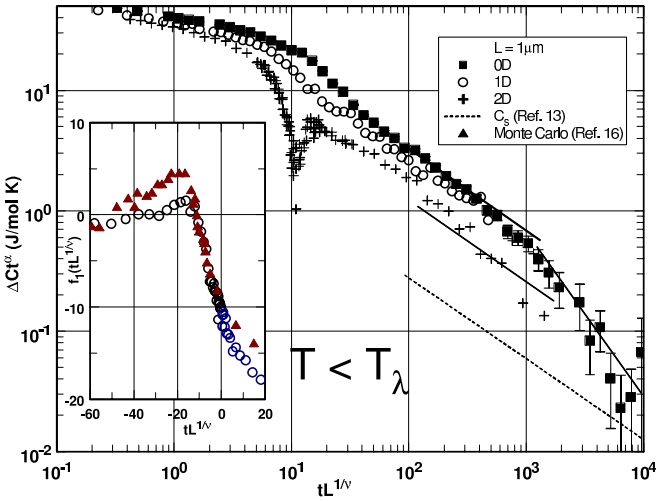

FIG. 3: The difference in the specific heat of confined helium from the bulk for $T < T_\lambda$ plotted according to Eq. 1. L is in Å. The solid lines through the data are drawn with slopes corresponding to the surface and edge specific heat, Eqs. 3, 4. The dashed line is a theoretical prediction for the surface region. The inset shows the data, plotted according to Eq. 2, for the channel geometry compared with a theoretical calculation for the same geometry. For the inset the reduced temperature is taken as negative for the region below T_λ.

to Eq. 4 one expects the surface contribution between the three geometries to be in the ratio of 1:2:3.

In Fig. 2 we show data for $T > T_\lambda$ plotted as $\Delta C t^\alpha$ versus the scaling variable $tL^{1/\nu}$. For the planar confinement we use the results of Ref. [9] (see also Ref. [14]) which comprises a series of measurements for *various* planar confinements which were shown to display universal data collapse. To calculate ΔC we use the bulk specific heat representation obtained in Ref. [8]. The measured heat capacity is normalized to the bulk data in the region above T_λ where finite-size effects are negligible, $t \gtrsim 10^{-2}$. The trend in the data in Fig. 2 shows the behavior expected from Eqs. 1, 3, 4. At large $tL^{1/\nu}$, the channel and boxes data show the effect of the edge specific heat: $\Delta C t^\alpha$ is consistent with a power-law behavior of -2ν, the solid lines. At intermediate $tL^{1/\nu}$, the surface specific heat dominates hence the exponent is $-\nu$, the dashed lines. For smaller $tL^{1/\nu}$, one picks up the full finite-size effects as $\Delta C t^\alpha$ "rolls over" to a much weaker temperature dependence. The data for 2D confinement have a well defined region where the surface specific heat dominates (there are no edge effects for this geometry), while the boxes and channels have at best a transition region between the edge specific heat and the fully developed finite-size effects. One can contrast the behavior of the present 1D data to those with a cylindrical geometry [15]. For the latter, the surface specific heat region extends to $tL^{1/\nu} = 10^4$, with no evidence of a change in power law. This is expected, long cylinders have a negligible edge contribution which comes from its ends; thus, one can take $g_e \approx 0$.

The equivalent plot for the region $T < T_\lambda$ is shown in Fig. 3. Here the data show more structure because of the specific heat maximum. In particular one notes that the data for 2D confinement have a very striking minimum on this plot compared with more subtle changes of curvature for the 1D and 0D confinements. It seems likely that this difference for 2D is a reflection of KT behavior. Also drawn on this plot are lines corresponding to the behavior of the surface and edge specific heats. The data for 1D confinement could not be obtained into the edge region because of the onset of a superfluid resonance.

Also, as an inset in Fig. 3, we show a comparison of the 1D data with a Monte Carlo calculation of $f_1(x)$ [16]. The theory is in good agreement with the data except near the specific heat maximum. Here the theory *exceeds* the maximum indicating that it does not capture the full import of confinement. In a similar comparison for 2D confinement, the theoretical maximum also exceeds the locus of the data [9]. A field theory calculation of A_s for planar confinement is shown as a dashed line [13]. For the channel and box geometries one would position this line respectively a factor of 2, and 3 higher. In all cases this line lies *below* the respective data. By contrast, above T_λ, one has *excellent agreement* with theory[9, 14], see Table I. We have also compared the 0D data with recent Monte Carlo calculations [17]. Excellent agreement is found for temperatures above the specific heat maximum.

To compare the magnitude of the surface and edge specific heat we have collected in Table I values of A_s^+, A_s^-, A_e^+, A_e^-, as well as the overall prefactor ratios for various geometries. The $+$, $-$ refer to $T > T_\lambda$ and $T < T_\lambda$, respectively. The amplitudes, which are independent of

TABLE I: Specific heat amplitudes and ratios for surface and edge specific heats. A_s and A_e are in units of JÅ/mol K, and JÅ^2/mol K respectively. The numbers in parenthesis are the expected ratios for the geometric factors.

	Surface: $T > T_\lambda$	Surface: $T < T_\lambda$	Edge: $T > T_\lambda$	Edge: $T < T_\lambda$
$\frac{channel}{planar}$	1.5 ± 0.1 (2)	2.0 ± 0.1 (2)	—	—
$\frac{box}{planar}$	2.1 ± 0.1 (3)	2.7 ± 0.2 (3)	—	—
$\frac{box}{channel}$	1.4 ± 0.1 (1.5)	1.3 ± 0.1 (1.5)	1.8 ± 0.2 (1-2)	—
Amplitude (Exp.)	$A_s^+ = -5.9 \pm 0.2$	$A_s^- = -8.6 \pm 0.5$	$A_e^+ = -370 \pm 40$	$A_e^- = -1100 \pm 110$
Amplitude (Theory)	$A_s^+ = -5.7$	$A_s^- = -2.0$	—	—

geometry, can be compared with theory where available. The ratios of the prefactors should yield the expected geometric ratios. One can see from this Table that these ratios are in agreement with expectations except for some of the surface terms for $T > T_\lambda$. Here the ratios *channel/planar* and *box/planar* are shy of the expected values 1.5 ± 0.2 vs. 2, and 2.1 ± 0.1 vs. 3. It seems likely that this is a reflection of the rather limited region in which the surface term is manifest for the box and channel geometry. The magnitude of A_s^+ is in excellent agreement with theoretical calculations, as has already been pointed out in [9, 14]. For A_s^- however, there is a strong disagreement with theory. This is true for 2D, 1D, and 0D confinements. While the theoretical values of A_s are from a first order calculation, and are not expected to be very accurate[13], it is nevertheless interesting that it is on the superfluid side that one finds disagreement. This is also the region, at least for 2D, where one finds the data for various L's do not scale [9]. The edge amplitudes have not been calculated theoretically for a system such as helium. We believe these are the first measurements near a critical point to identify such contribution.

In summary, we have presented data of the specific heat of helium confined at the same smallest dimension but with different dimensionality crossover. This demonstrates for the first time the role of the lower dimension for the same small confinement L. We have also identified surface, and for the first time, edge contributions to finite-size effects. Comparison with theory shows agreement in some aspects and disagreement in others.

We acknowledge the support of the National Science Foundation, DMR 9972287, DMR 0242246, and the Cornell Nanofabrication Facility, 526-94.

[1] See for instance Shang-Keng Ma *Modern Theory of Critical Phenomena* (Benjamin/Cunnings,1981).
[2] M. E. Fisher, in *Critical Phenomena*, Proc. 51st "Enrico Fermi" Summer School, Varenna, Italy (M. S. Green, ed. Academic Press, NY, 1971), see also M. E. Fisher and M. N. Barber, Phys. Rev. Lett., **28**, 1516 (1972).
[3] V. Privman, *Finite Size Scaling and Numerical Simulations of Statistical Systems* (World Scientific, NJ, 1990), see in particular, eqs. 2.28 and 2.41-2.42.
[4] See for instance G. Ahlers in *The Physics of Liquid and Solid Helium.* (K. H. Bennemann and J. B. Ketterson eds, J. Wiley, New York 1976).
[5] J. M. Kosterlitz and D. J. Thouless, *J. Phys C* **6**, 1181 (1973).
[6] I. Rhee, D. J. Bishop, A. Petrou, and F. M. Gasparini, Rev. Sci. Instrum. **61**, 1528 (1990).
[7] The helium in the connecting lines represents 1.8% by volume of the total sample in the cell. However, due it its small spatial confinement, 0.018 μm $\times$ 1 μm, we find that it contibutes negligiblely to the heat capacity.
[8] S. Mehta, M. O. Kimball, and F. M. Gasparini, J. Low Temp. Phys. **114 (**Nos.) 5/6, 467 (1999).
[9] M. O. Kimball, S. Mehta, and F. M. Gasparini, J. Low Temp. Phys. **121** Nos. **1/2**, 29 (2000).
[10] For a review of finite-size scaling see, M. N. Barber in *Phase Transitions and Critical Phenomena*, C. Domb and J. L. Lebowitz vol. **8** (Academic Pres, NY, 1983); V. Privman, Ref. [3].
[11] The exponents α and ν have been obtained in a variety of experiments and theoretical calculations. For the latest experimental determinations see J. Lipa, D. R. Swanson, J. A. Nissen, T. C. P. Chui and U. Israelsson, Phys. Rev. Lett. **76**, 944 (1996); L. S. Goldner, N. Mulders and G. Ahlers, J. Low Temp. Phys. **93**, Nos. 1/2, 131 (1993); for theory see M. Campostrini, A. Pelissetto, P. Rossi and E. Vicari, Phys. Rev. B **61**, 5905 (2000).
[12] R. Schmolke, A. Wacker, V. Dohm, and D. Frank, Physica B **575**, 165 (1990), see also, V. Dohm, Physica Scripta vol. **T49**, 46-58 (1993).
[13] U. Mohr and V. Dohm, Physica B **284-288**, 43 (2000).
[14] J. A. Lipa and *et al.*, Phys. Rev. Lett. **84**, 4894 (2000).
[15] J. A. Lipa, M. Coleman, and D. A. Stricker, *J. Low Temp. Phys.* **124, (**Nos.) 3/4, 443 (2001).
[16] N. Schultka and E. Manousakis, J. Low Temp. Phys. **111, Nos. (5/6)**, 783 (1998).
[17] K. Nho and E. Manousakis, Phys. Rev. B **68**, 174503 (2003).